

See discussions, stats, and author profiles for this publication at: <https://www.researchgate.net/publication/47542948>

Reliability and Storage Capacity: a Compromise Illustrated in the Two-Step Spin-Crossover System [Fe(bapbpy)(NCS)(2)]

ARTICLE *in* INORGANIC CHEMISTRY · OCTOBER 2010

Impact Factor: 4.76 · DOI: 10.1021/ic101669b · Source: PubMed

CITATIONS

14

READS

35

8 AUTHORS, INCLUDING:



José Sánchez Costa

Laboratoire de Chimie de Coordination.

73 PUBLICATIONS 1,490 CITATIONS

[SEE PROFILE](#)



Boris Le Guennic

Université de Rennes 1

137 PUBLICATIONS 2,367 CITATIONS

[SEE PROFILE](#)



Sylvestre Bonnet

Leiden University

60 PUBLICATIONS 1,009 CITATIONS

[SEE PROFILE](#)



Jan Reedijk

Leiden University

1,375 PUBLICATIONS 38,115 CITATIONS

[SEE PROFILE](#)

Reliability and Storage Capacity: a Compromise Illustrated in the Two-Step Spin-Crossover System [Fe(bapbpy)(NCS)₂]

Mikael Kepenekian,[†] José Sánchez Costa,^{*,‡} Boris Le Guennic,[†] Pascale Maldivi,[§] Sylvestre Bonnet,[⊥] Jan Reedijk,^{⊥,▽} Patrick Gamez,^{*,#} and Vincent Robert^{*,†,○}

[†]Laboratoire de Chimie, Ecole Normale Supérieure de Lyon, CNRS, Université de Lyon, 46 allée d'Italie, 69364 Lyon Cedex 07, France, [‡]Grup de Magnetisme i Molecules Functionales (GMMF), Departament de Química Inorgànica, Universitat de Barcelona, Diagonal 647, 08028 Barcelona, Spain, [§]Laboratoire de Reconnaissance Ionique et Chimie de Coordination, UJF, UMR_E 3 CEA-UJF, CNRS, FRE 3200, 17 rue des Martyrs, F-38054 Grenoble Cedex 9, France, [⊥]Leiden Institute of Chemistry, Leiden University, P.O. Box 9502, 2300 RA Leiden, The Netherlands, [#]Universitat de Barcelona, Martí i Franquès 1-11, 08028 Barcelona, Spain and Institució Catalana de Recerca i Estudis Avançats (ICREA), Barcelona, Spain, [▽]Department of Chemistry, King Saud University, P.O. Box 2455, Riyadh 11451, Saudi Arabia, and [○]Laboratoire de Chimie Quantique, Institut de Chimie UMR 7177 - CNRS/Université de Strasbourg, 4 rue Blaise Pascal B.P. 1032, 67070 Strasbourg, France

Received August 17, 2010

The design of bistable magnetic systems should enable the storage of information by manipulation of the spin degrees of freedom. However, such a strategy relies on the preparation of target objects, whose environment must be controlled to favor a hysteretic behavior. Here, we report the successful modeling of a highly cooperative two-step spin-crossover iron(II) compound, [Fe(bapbpy)(NCS)₂]. The magnetic susceptibility measurements and low- and high-temperature hysteretic cycles reflect the presence of an intermediate phase, which controls the memory-storage capacity of this material. It is shown that the hysteresis loop widths can be traced theoretically by evaluating the electrostatic contributions between the transiting units. Despite the apparent reduction of intermolecular interactions upon cooling, it is suggested that the enhanced fluctuations of the Madelung field are responsible for the observed hysteresis width changes. This counterintuitive scenario makes the preparation of information storage devices an even more challenging task, where theoretical inspections are very insightful.

Introduction

Magnetic systems provide the opportunity to manipulate the spin degrees of freedom. There has been considerable interest for spin bistability,^{1,2} because potential applications to generate electronic devices, such as information storage media, may be anticipated.³ One of the most spectacular examples is the spin-crossover (SCO) phenomenon, which would enable the use of molecular-based materials as memory devices and molecular switches. Besides, recent proposals suggest that iron(II) coordination compounds can serve as

useful units for quantum manipulation.^{4–6} Their ability to evolve between two states under some external stimuli (temperature, pressure, light irradiation, and magnetic field)² is a prerequisite, which is here achieved with the existence of a low-spin state ($S = 0$) and a high-spin state ($S = 2$). However, such applications require the occurrence of a hysteresis loop, characterized by a difference in the transition temperatures between the cooling and warming modes (namely, T_1 and T_1 ; see Figure 1). Indeed, a hysteresis loop allows for two different states being possibly populated at a given temperature. In order to build up permanent and reliable memories, one should aim at materials holding sufficiently wide loops around room temperature. Such demand calls for a detailed understanding of the hysteresis phenomenon, which could be turned into predictions for the preparation of target objects.

The need for cooperative SCO materials has led to extensive experimental efforts aimed at the design of specific

*To whom correspondence should be addressed. E-mail: jose.sanchezcosta@qi.ub.es (J.S.C.), patrick.gamez@qi.ub.es (P.G.), vincent.robert@ens-lyon.fr (V.R.).

(1) Kahn, O.; Launay, J.-P. *Chemtronics* **1988**, 3, 140–151.
(2) Gutlich, P.; Goodwin, H. A. Spin crossover—An overall perspective. *Spin Crossover in Transition Metal Compounds I*; Springer-Verlag: Berlin, 2004; Vol. 233, pp 1–47.

(3) Letard, J. F.; Guionneau, P.; Goux-Capes, L. Towards spin crossover applications. *Spin Crossover in Transition Metal Compounds III*; Springer-Verlag: Berlin, 2004; Vol. 235, pp 221–249.

(4) Cobo, S.; Molnar, G.; Real, J. A.; Bousseksou, A. *Angew. Chem., Int. Ed.* **2006**, 45, 5786–5789.

(5) Alam, M. S.; Stocker, M.; Gieb, K.; Muller, P.; Haryono, M.; Student, K.; Grohmann, A. *Angew. Chem., Int. Ed.* **2010**, 49, 1159–1163.

(6) Chandrasekar, R.; Schramm, F.; Fuhr, O.; Ruben, M. *Eur. J. Inorg. Chem.* **2008**, 2649–2653.

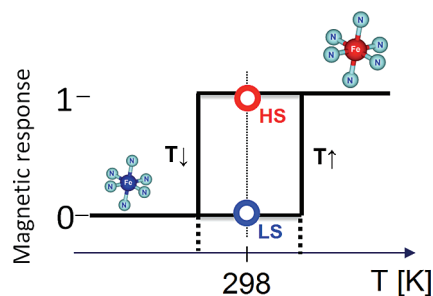


Figure 1. Temperature-induced SCO phenomenon and hysteretic behavior in an iron(II)-based material. The magnetic response corresponds to the magnetization with respect to its high-temperature value, featuring the molar fraction of HS complexes.

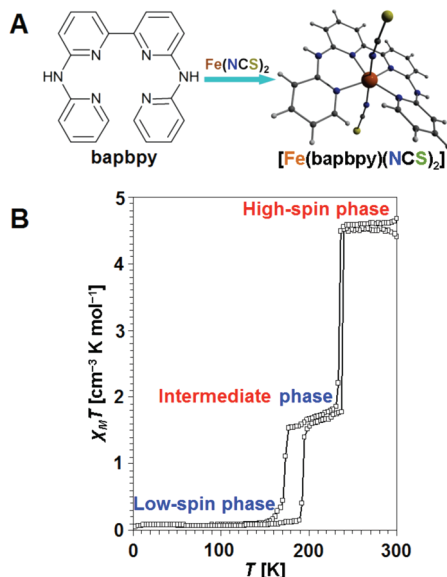


Figure 2. (A) Compound **1**, obtained from $\text{Fe}(\text{NCS})_2$ and the ligand bapbpy. (B) Magnetic behavior of **1** as a $\chi_M T$ vs T plot.⁸ The high $\chi_M T$ value (larger than the expected $3 \text{ cm}^3 \cdot \text{K} \cdot \text{mol}^{-1}$) is explained by the orientation effects of the polycrystalline compound **1**.

weak-interaction networks (van der Waals), thus calling for different chemical-engineering strategies.⁷ One promising route is to take advantage of the flexibility of molecular chemistry to set up the desired bistability and hysteresis behaviors. Nevertheless, the coexistence of different interactions within the materials makes the predictive character a much-discussed issue. Information and interpretations can be extracted a posteriori from X-ray measurements, assuming that the high- and low-temperature data can effectively be collected. A clear understanding, starting from the constitutive units up to the crystal structure, is undoubtedly required to design appropriate objects. Therefore, interplay between synthetic chemists, spectroscopists, and theoreticians is of prime importance to control these microscopic and macroscopic aspects.

The present study is devoted to the rationalization of the hysteretic behavior observed in a mononuclear Fe^{II} coordination material (see Figure 2), $[\text{Fe}(\text{bapbpy})(\text{NCS})_2]$ (**1**).⁸ This system is particularly attractive because of the presence of two hysteretic loops, reproducible over six cooling/heating

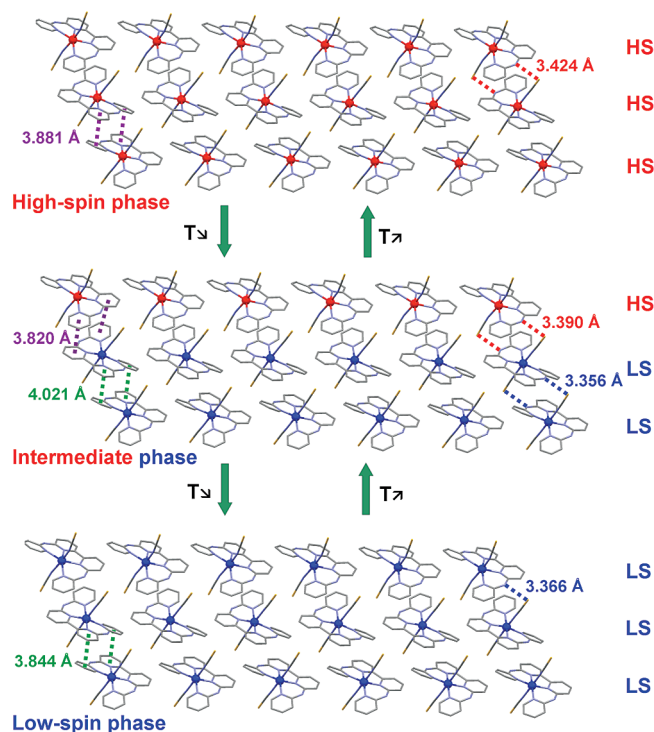


Figure 3. Temperature-induced SCO in **1**, characterized by LS, IP, and HS phases. The red and blue dotted lines symbolize $\text{N}-\text{H} \cdots \text{S}$ hydrogen bonds, and the green and purple dotted lines indicate $\pi-\pi$ interactions. The IP exhibits a 1:2 ratio of HS and LS centers.

cycles, with available X-ray diffraction data for the three relevant phases, namely, the low-spin (LS), high-spin (HS) and intermediate (IP) phases (see Figure 2). The most striking features in **1** are the following: (i) the IP dominates over a wide range of temperatures, and (ii) this phase is not simply a random mixture of the HS and LS ones, but it has a specific signature by Raman spectroscopy and X-ray crystallography (see Figure 3).^{8,9} Therefore, the bistability in **1** may be exploited for multiple data storage with detection at two different temperatures. The origins of this intriguing scenario remain unravelled, while its interpretation should provide important conceptual ideas for future research investigations. The origin of the different hysteresis widths has been clarified using combined magnetic susceptibility simulations and ab initio calculations. These theoretical studies suggest that an elastic-based justification fails to account for the cooperative behavior of **1**.

Computational Details

We used a wave-function-based correlation method (complete active space self-consistent field, CASSCF) to investigate the energetics and charge redistribution effects in the molecular structure of **1**. This method, which uses the exact Hamiltonian, has proven to be very effective in the evaluation of charge redistributions.^{10,11} However, the active space should not be limited to the d-type orbitals but should be extended to account for the important charge fluctuations accompanying the $S = 0 \rightarrow S = 2$ spin change. Thus, the active space that we used

(7) Itkis, M. E.; Chi, X.; Cordes, A. W.; Haddon, R. C. *Science* **2002**, 296, 1443–1445.

(8) Bonnet, S.; Siegler, M. A.; Costa, J. S.; Molnar, G.; Bousseksou, A.; Spek, A. L.; Gamez, P.; Reedijk, J. *Chem. Commun.* **2008**, 5619–5621.

(9) Bonnet, S.; Molnar, G.; Costa, J. S.; Siegler, M. A.; Spek, A. L.; Bousseksou, A.; Fu, W. T.; Gamez, P.; Reedijk, J. *Chem. Mater.* **2009**, 21, 1123–1136.

(10) Sadoc, A.; Broer, R.; de Graaf, C. *J. Chem. Phys.* **2007**, 126, 134709.

(11) Banse, F.; Girerd, J. J.; Robert, V. *Eur. J. Inorg. Chem.* **2008**, 4786–4791.

consists of (i) the mainly Fe 3d character orbitals extended with a set of virtual orbitals of the same symmetry (so-called 3d' orbitals) and (ii) two occupied e_g -like symmetry orbitals with mainly ligand character (σ_1 and σ_2), leading to "10 electrons in 12 molecular orbitals (MOs)" (CAS[10,12]).¹² All atoms were depicted using available ANO-RCC primitive basis sets in the Molcas 7.0 package, contracted into [7s6p5d3f2g1h], [4s3p1d], and [3s2p1d] for the Fe, N, and C elements, respectively.¹³ A minimal basis set contraction [1s] was used for the H atoms. Then, the active MOs were relocated to grasp the importance of charge-transfer (CT) contributions concentrated into the wave-function expansion. Starting from a reference Fe d^6 picture based upon the relocated MOs, we looked into the CT configurations to evaluate the d-orbital occupancy in an orthogonal valence-bond-type analysis. In practice, the HS-state reference configuration d^6 reads $(d_{x^2-y^2})^1(d_{z^2})^1(\sigma_1)^2(\sigma_2)^2$ (i.e., no CT), while the leading CT configurations correspond to $(d_{x^2-y^2}, d_{z^2})^3(\sigma_1, \sigma_2)^3$ (i.e., simple CT) and $(d_{x^2-y^2}, d_{z^2})^4(\sigma_1, \sigma_2)^2$ (i.e., double CT). These configurations correspond to formal d^7 and d^8 configurations for the Fe center, respectively. In contrast, the reference configuration in the LS state is $(d_{x^2-y^2})^0(d_{z^2})^0(\sigma_1)^2(\sigma_2)^2$. Thus, the following electronic configurations $(d_{x^2-y^2}, d_{z^2})^1(\sigma_1, \sigma_2)^3$ and $(d_{x^2-y^2}, d_{z^2})^2(\sigma_1, \sigma_2)^2$ were considered for the LS state. The weights of the successive CT mixing into the reference Fe d^6 configuration were evaluated from the reading of the wave function to quantify the point charges upon the Fe and N centers.

Results and Discussion

To account for the presence of a hysteretic behavior, the Slichter and Drickamer's thermodynamic model¹⁴ introduces a cooperativity factor Γ in the derivation of the Gibbs potential G with respect to the HS molar fraction x :

$$G = x(\Delta H - T\Delta S) + RT[\ln(1-x) + (1-x)\ln(1-x)] + \Gamma x(1-x) \quad (1)$$

$$\ln[(1-x)/x] = [\Delta H + \Gamma(1-2x) - T\Delta S]/RT \quad (2)$$

Γ aims at representing the effective interaction between HS and LS centers. This approach does not rely upon any assumption upon the crystal structure but aims at determining the relevant thermodynamic parameters. One important issue is indeed the definition of an appropriate model in the presence of the IP. Structural and spectroscopic observations demonstrate that the latter is characterized by two-thirds of the LS Fe^{II} centers and one-third of the HS centers (see Figure 3). Nevertheless, no spectacular cooperativity change, which would support an enhancement of the hysteresis loop at low temperature, accompanies the evolution of the three-dimensional network along the transition. To what extent can one anticipate the hysteresis widths from analysis of the crystal structure? Besides, can one interpret the compromise between the number of transiting sites and the hysteresis width? To answer these questions, the magnetic susceptibility variations have first been examined in detail to appraise the specific features of this two-step SCO phenomenon. In fact, this system affords memory storage at two different

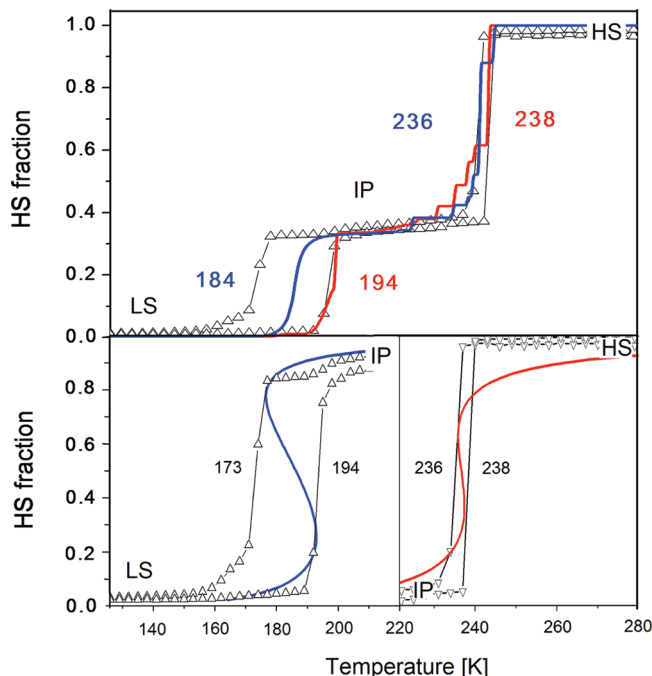


Figure 4. χT variations with respect to the temperature. $T_1 = 183$ K and $T_2 = 237$ K correspond to the LS \rightarrow IP and IP \rightarrow HS experimental transition temperatures. The triangles symbolize the experimental values. Solid lines correspond to the fit considering dependent (top graph) and independent (bottom graph) SCO phenomena in **1**.

Table 1. Macroscopic Quantities ΔH_1 and ΔH_2 ($\text{kJ}\cdot\text{mol}^{-1}$) and ΔS_1 and ΔS_2 ($\text{J}\cdot\text{mol}^{-1}\cdot\text{K}^{-1}$) Resulting from DSC Measurements⁸ and the Spin-Independent Model

	ΔH_1	ΔH_2	ΔS_1	ΔS_2
experiment	9.7(5)	17(2)	48(6)	72(8)
"spin-independent" fit	9.50	17.7	51	75

temperatures, with different capacities reflected from the crystal changes (see Figure 3). Next, a microscopic inspection has been carried out using rigorous quantum chemical calculations to rationalize the width of the hysteresis cycles.

We modeled the presence of the plateau following two different strategies. In a first approach, we defined two nonindependent subsets of Fe centers inside the material.¹⁵ Thus, the total HS molar fraction of the system can be expressed as a weighted average of the molar fractions x_1 and x_2 of each subset, $x = (1-c)x_1 + cx_2$. From the structural data (see Figure 3), the weighting coefficient c is $1/3$, as exhibited by the IP. At the thermodynamic equilibrium, a set of coupled equations similar to eq 2 is obtained as a function of the different cooperativity factors. The main difference with eq 2 lies in the introduction of supplementary Γ_{12} and Γ_{21} parameters accounting for the interaction between Fe centers belonging to different subsets. Figure 4 (top) shows the simulated curve, setting $\Gamma_{12} = \Gamma_{21}$, and using the available experimental values of ΔH_1 , ΔH_2 , ΔS_1 , and ΔS_2 (see Table 1).⁸ The resulting optimized cooperativity factors Γ_{11} and Γ_{22} are 450 and 458 K, respectively, while $|\Gamma_{12}|$ and $|\Gamma_{21}|$ are less than 10 K. Clearly, a significant deviation is observed between the experimental curve and the simulated one (see Figure 4, top): the hysteresis width is too narrow in the low-temperature

(12) Kepenekian, M.; Robert, V.; Le Guennic, B.; de Graaf, C. J. *Comput. Chem.* **2009**, *30*, 2327–2333.

(13) Karlström, G.; Lindh, R.; Malmqvist, P. A.; Roos, B. O.; Ryde, U.; Veryazov, V.; Widmark, P. O.; Cossi, M.; Schimmelpfennig, B.; Neogrady, P.; Seijo, L. *Comput. Mater. Sci.* **2003**, *28*, 222–239.

(14) Slichter, C. P.; Drickamer, H. G. *J. Chem. Phys.* **1972**, *56*, 2142–2160.

(15) Niel, V.; Thompson, A. L.; Goeta, A. E.; Enachescu, C.; Hauser, A.; Galet, A.; Munoz, M. C.; Real, J. A. *Chem.—Eur. J.* **2005**, *11*, 2047–2060.

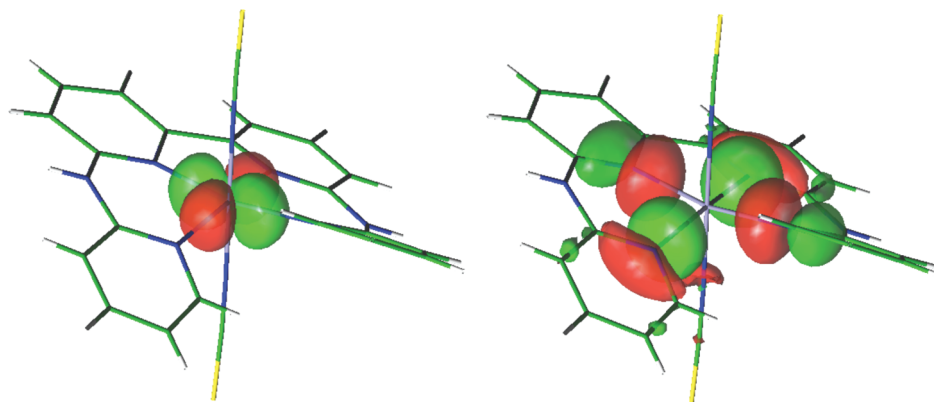


Figure 5. Selection of localized MOs used to quantify CTs. Upon the $S = 0 \rightarrow S = 2$ spin change in the $\text{Fe}(\text{bapbpy})(\text{NCS})_2$ compound **1**, a net calculated $\Delta Q = 0.64 e^-$ metal-to-ligand CT occurs.

regime. As a major conclusion, this model does not offer a satisfactory simulation of the two-step behavior observed in **1**.

Considering the negligible value of the intersubset interactions, we asserted in a second approach that the two SCO steps were independent, referred to as systems Σ_1 and Σ_2 . Therefore, the IP plays a dual role along this description. In the heating mode, it is considered to be the “high-temperature” phase for the first transition, whereas it behaves as the “low-temperature” phase for the second transition. This model provides a better agreement between simulated and experimental data (see Figure 4, bottom). First, the extracted cooperativity factors Γ_{Σ_1} and Γ_{Σ_2} are almost identical (~ 510 K), but a nonnegligible enhancement ($\sim 10\%$) is measured as compared to Γ_{11} and Γ_{22} . The observed reduction of the hysteresis widths upon heating can thus be attributed to the difference between the transition temperatures, $T_1 = 183$ K and $T_2 = 237$ K. Indeed, the hysteresis width is governed by the ratio between the cooperativity factor and the transition temperature. The relevance of this second picture is also supported by the extracted thermodynamic information (see Table 1), which compares favorably with the experimental values obtained from differential scanning calorimetry (DSC).⁸ From this inspection, we can conclude that **1** should be considered as two independent SCO systems, Σ_1 and Σ_2 .

The puzzling result $\Gamma_{\Sigma_1} \sim \Gamma_{\Sigma_2}$ in **1** deserves particular theoretical attention. Indeed, the magnetic behavior is rather intriguing because one might have expected a different scenario from the crystallographic changes (see Figure 3). As a matter of fact, the transiting rows in the $\text{LS} \rightarrow \text{IP}$ transition are almost noninteracting, whereas they form pairs in the $\text{IP} \rightarrow \text{HS}$ transition. Because the origin of cooperativity is traditionally attributed to the elastic contributions (i.e., $\Gamma = \Gamma_{\text{elastic}}$), one would anticipate $\Gamma_{\Sigma_2} > \Gamma_{\Sigma_1}$. This result is clearly in contradiction with our previous fit, which concluded upon $\Gamma_{\Sigma_1} \sim \Gamma_{\Sigma_2}$. Part of the answer is to be found in our recent works. Indeed, we have recently shown that the electrostatic effects in the crystal, known as the Madelung field, are likely to polarize the Fe–N bonds during the transition.^{16,17} To account for the hysteresis growth, it is necessary to include a supplementary polarization contribution (Γ_{pol}), leading to $\Gamma = \Gamma_{\text{elastic}} + \Gamma_{\text{pol}}$. In contrast with

Table 2. Calculated Atomic Charges upon the Fe and N Atoms Belonging to the SCN^- Ligands^a

	LS	HS
Fe	1.25	1.89
N	−0.88	−1.20

^a The changes of the bapbpy N charges are negligible.

Γ_{elastic} , not only can a physical understanding of Γ_{pol} be given, but also an evaluation through ab initio calculations is accessible. Charge redistribution occurs at a microscopic level during the $\text{LS} \rightarrow \text{HS}$ transition, which modulates the macroscopic Madelung field. This phenomenon is qualitatively understood from the occupations of antibonding MOs in the $S = 2$ spin state. Because these MOs are mostly localized on the N atoms, a net metal-to-ligand CT ΔQ is expected. Such a phenomenon can be quantified using a valence-bond-type analysis based upon localized MOs (see Figure 5).

We have performed ab initio CASSCF calculations upon the individual $\text{Fe}(\text{bapbpy})(\text{NCS})_2$ unit to quantitatively evaluate the electronic density and estimate point charges upon the Fe and N atoms (see Table 2). Such an approach affords a well-balanced description of charge redistributions within the complex. Density functional theory based methods might not be adapted for such purposes because they are known to suffer from (i) the systematic self-interaction error and (ii) the arbitrariness of the exchange-correlation potential. The magnitudes of the point charges along with the crystallographic positions afford an evaluation of the Madelung field acting upon the Fe^{II} and N centers (see Table 3).¹⁶ Considering the electronic density reorganization within each building block of the network between the LS and HS states, the potential generated by an assembly of HS centers differs from the one resulting from a collection of LS species. A mean-field approach leads to the following expression for the cooperativity parameter:

$$\Gamma_{\text{pol}} = \Delta Q(\delta V_{\text{HS}} - \delta V_{\text{LS}}) \quad (3)$$

where δV_{HS} and δV_{LS} stand for the difference of the potential upon the Fe and N atoms in the HS and LS phases, respectively.¹⁶ Because the polarization contributions to cooperativity are proportional to the charge fluctuations, Γ_{pol} is only sensitive to atoms whose charges are modified along the transition. From our calculations, only the Fe and thiocyanate

(16) Kepenekian, M.; Le Guennic, B.; Robert, V. *Phys. Rev. B* **2009**, 79.

(17) Kepenekian, M.; Le Guennic, B.; Robert, V. *J. Am. Chem. Soc.* **2009**, 131, 11498–11502.

Table 3. Calculated Variations of the Potential Differences $\delta V = \delta V_{\text{Fe}} - \delta V_{\text{N}}$ (a.u.) Resulting from the Madelung Field Fluctuations along the Successive LS \rightarrow IP and IP \rightarrow HS Transitions

	LS \rightarrow IP	IP \rightarrow HS
$\Delta(\delta V) (10^3)$	-5.16	-4.98

N charges evolve sensitively. Therefore, the charges upon all of the other atomic positions, including the Fe nearest-neighbor bapbpy N atoms, are not relevant for the present evaluation of Γ_{pol} . From our previous inspection, **1** should be considered as two independent SCO systems. Thus, two cooperative factors are introduced as a consequence of the dual role played by the IP. From the combination of our *ab initio* calculations and the crystallographic data available for the three phases, we have found that the LS \rightarrow IP Γ_{pol} parameter is 326 K, whereas it is only 190 K for the IP \rightarrow HS one. This analysis stresses the importance of the electrostatic effects in the growth of hysteresis loops. Thus, the cooperativity cannot be limited to a purely elastic picture. Quantitatively, $\Gamma_{\text{elastic}} = \Gamma - \Gamma_{\text{pol}}$ is evaluated to be 184 K for the LS \rightarrow IP transition and 320 K for the IP \rightarrow HS one. First, the elastic and polarization components are comparable in amplitude. Then, these figures are consistent with the structural changes, which suggest an enhanced cooperativity network upon heating. Importantly, the crucial role played by the polarization effects offers reconciliation between the intuitive approach based on crystal engineering and the purely elastic modeling of cooperative effects, which is not satisfactory for compound **1** (see Figure 6). The classical crystal engineering approach is based on the idea that supramolecular interactions, such as hydrogen bonds and π - π stacking, promote cooperative behaviors and hysteresis loops through purely elastic interactions. Thus, the structural changes associated with the SCO of each molecule (i.e., the Fe-N bond distances differ between the HS and LS states) are transmitted mechanically from neighbor to neighbor. For compound **1**, the expected trend is only found when comparing Γ_{elastic} (see Figure 6). In our model, cooperative effects also originate from the Madelung fields created by the crystallographic phase around each molecule. This Madelung field is difficult to predict by crystal engineering, but it can be quantitatively calculated when the X-ray structure of the material is known, which allows evaluation of the elastic contribution as well. For compound **1**, the polarization contribution Γ_{pol} follows an inverse trend compared to Γ_{elastic} (see Figure 6), which leads to similar values for Γ of both transitions and, hence, to a thinner hysteresis loop for the high-temperature transition. Thus, this analysis sheds another view

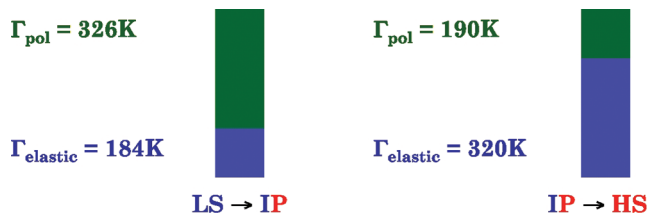


Figure 6. Split cooperativity parameter Γ into elastic (Γ_{elastic}) and polarization contributions (Γ_{pol}) for both LS \rightarrow IP and IP \rightarrow HS steps.

on the intriguing SCO phenomenon, where short- and long-range interactions compete. It also affords a satisfying rationalization of the macroscopic behavior of compound **1**.

Conclusions

In summary, we propose a model of the hysteretic two-step behavior in compound **1**. The interplay between the experimental and theoretical approaches has led to a thorough understanding of the mechanisms governing the hysteresis loop formation. In the light of our analysis, this material should be considered as two independent SCO systems based upon the same constitutive unit. The initial contradiction arising from the higher number of transiting molecules in the high-temperature transition, and the reduced hysteresis width, illustrates the limitations of a purely elastic approach to cooperativity. The electrostatic contributions, which can be evaluated from *ab initio* calculations, stress another important physical origin of spin bistability. Thus, the challenging control of the cooperativity remains a critical issue because the hysteresis phenomenon cannot be limited to a single well-defined physical effect.

Interestingly, the cooperativity factor in **1**, a critical feature for the information storage reliability, decreases, while the storage capacity, featured by the number of transiting sites, increases. The present competition can be considered as a manifestation of a fundamental physical behavior. Such an observation is additional evidence that reliability is not an extensive property in information storage devices. Quite remarkably, the challenging compromise between reliability and storage capacity is reflected in this two-step SCO system.

Acknowledgment. M.K., B.L., and V.R. thank the ANR project “fdp magnets” for financial support. J.S.C. acknowledges the Spanish Ministerio de Ciencia through the Juan de la Cierva Program (18-08-463B-750).